Cyclic fatigue of a mica-containing glass-ceramic at Hertzian contacts

Hongda Cai,[a] Marion A. Stevens Kalceff,[b] Bryan M. Hooks,[c] and Brian R. Lawn
Materials Science and Engineering Laboratory, National Institute of Standards and Technology, Gaithersburg, Maryland 20899

Kenneth Chyung
Corning Incorporated, Sullivan Park, Corning, New York 14830

(Received 10 January 1994; accepted 27 May 1994)

Fatigue damage in a mica-containing glass-ceramic is examined using Hertzian contact tests. For the material in its base glass state, such tests indicate that fatigue occurs solely by chemically enhanced cone crack extension. In the glass-ceramic, fatigue is evident as an expansion of a macroscopic subsurface microfracture zone. Comparative observations of the subsurface damage in static and cyclic loading, and tests in different environments, indicate that the fatigue in the glass-ceramic is mechanical in origin, although it is enhanced by moisture. This result is reinforced by load-point-displacement data, which reveal significant hysteresis in the glass-ceramic but not in the base glass. Flexure tests on Hertz-indented glass-ceramic specimens show only a slight loss of strength, $<5\%$, over 10^5 cycles. This contrasts with the base glass which, although of higher laboratory strength, is subject to abrupt and severe strength degradation from cone crack pop-in. High magnification examination of the subsurface damage in the glass-ceramic suggests the underlying cause of the mechanical fatigue mechanism to be attrition of frictional tractions at closed microcrack interfaces.

I. INTRODUCTION

In a recent study we described the nature of damage that occurs beneath a Hertzian indenter in a mica-containing machinable glass-ceramic.[1] There we showed that, relative to the base glass state, the glass-ceramic deforms relatively easily, in a "pseudo-ductile" mode. In the base glass classical Hertzian cone cracks form in the weak tensile zone outside the contact circle. In the glass-ceramic there is a transition to accumulated subsurface damage in the strong shear-compression zone below the contact. The difference in response is attributed to the presence of mica flakes from crystallization during heat treatment of the glass matrix. The flakes provide discrete weak interfaces, which deform in shear and initiate microcracks at their edges. This short-crack weakness accounts for the machinability.

Mica-containing glass-ceramics are of interest here for their use as model two-phase brittle materials. Notwithstanding their machinability,[2,3] they have respectable toughness in the long-crack region.[4] On the other hand, little is known about their lifetime characteristics in cyclic stressing. Long-term engineering design with these materials in certain applications (bearings, dental restorations, etc.) requires knowledge of the fatigue characteristics, especially in concentrated loading.

Accordingly, the aim of the present work is to examine the contact fatigue behavior of the same mica-containing glass-ceramic as used in our preceding single-cycle study.[1] The material is subjected to cyclic Hertzian contacts, in controlled environments, and the ensuing subsurface microfracture pattern followed as a function of number of cycles. Comparative tests on the base glass establish a reference baseline for materials with well-defined macrocracks. Load-point-displacement measurements are made to determine the extent of mechanical hysteresis in the contact cycle. Strength tests on indented flexure specimens provide a quantitative measure of loss of mechanical integrity arising from the cyclic loading. Relative to the base glass, the glass-ceramic shows considerable damage accumulation from cyclic fatigue, but little strength loss, indicating an acquired damage-tolerance characteristic from the crystallization heat treatment. A possible micromechanical source of the fatigue will be considered.

II. EXPERIMENTAL

The material used in this study was a commercial mica-containing glass-ceramic, produced under the trade

[a]Guest Scientist on leave from Department of Materials Science and Engineering, Lehigh University, Bethlehem, Pennsylvania 18015.
[b]Guest Scientist on leave from Department of Applied Physics, University of Technology, Sydney, New South Wales 2007, Australia.
[c]Summer student from Harvard University, Cambridge, Massachusetts 02138.

name Macor (Corning Inc., Corning, NY), the same material as used in our previous study[1] on single-cycle damage. In its "green" glass form, the base material contains submicrometer-scale fluoride-rich droplets from liquid phase separation during the initial cooling process.[2] In its final heat-treated form, it contains ≈55% randomly oriented interlocking fluorophlogopite mica flakes 10 μm long and 1 to 2 μm thick in a matrix of ≈45% borosilicate glass.[2,3,5] The mica flakes with their weak basal cleavage and matrix interfaces facilitate easy fracture at the microstructural level, accounting for the machinability,[2] yet act as effective restraints on fracture at the macrostructural level, resulting in respectable long-crack toughness.[4]

Surfaces of plate specimens 25 mm square and 4 mm thick from blocks of mica-containing Macor and base glass were polished with diamond paste to 1 μm finish for testing in cyclic Hertzian loading.[6] Repeat loading on a spherical tungsten carbide indenter of radius r = 3.18 mm was delivered using a servo-hydraulic universal testing machine (Instron Model 8502, Instron Corp., Canton, MA). A transducer (LOCAN 320, Physical Acoustics Corp., Princeton, NJ) was used to monitor any acoustic activity during the tests. Load-point-displacement data were collected in some tests using a crack-opening displacement clip gauge mounted at one end on the specimen surface and at the other on the base of the shaft housing the indenting sphere, and analyzed on a data acquisition system.

For detailed microscopic investigation of the subsurface damage in the mica-containing glass-ceramic, two techniques, "section-and-etch" and "bonded-interface", were adopted. For the base material, a section-and-etch procedure previously developed for tracing the downward evolution of cone cracks in glass[7] proved most adequate. In this procedure, a row of indentations was made in the specimen surface and the specimen diamond-sawn normal to this surface and close to the line of centers through the indentations. The cut section was then ground and polished (1 μm finish) down to the line of centers. Traces of the cone cracks were revealed by etching the sectioned surface in 5% HF acid solution for 2 min. The section was lightly polished again to remove a slight roughness arising from the inhomogeneities in the glass, and gold coated prior to observation in reflected polarized illumination.

For the glass-ceramic, a bonded-interface specimen configuration was employed.[1,8] Two polished half-specimens were first clamped together with a thin layer (<10 μm) of cyanoacrylate-based adhesive (Loctite Corp., Newington, CT) to form a bonded interface, and the test surface ground and polished perpendicular to this interface. Cyclic Hertzian indentations were then made in a row along the interface trace at the test surface. The bonding adhesive was subsequently dissolved in acetone to separate the specimens. After coating the cleaned surfaces with gold, the (half) surface and subsurface damage was examined in reflection optical microscopy using Nomarski interference or polarized illumination.

A word may be said here about the choices of these two sectioning procedures for the two material forms. The section-and-etch technique is ideal for the base glass, where etching can highlight the crack traces without complication.[7] However, it is not suitable for the glass-ceramic, because the mica particles provide preferential etch sites, obscuring detail from the damage process. The bonded-interface technique is ideal for the glass-ceramic, because of its extreme sensitivity to small shear offsets on the section surface in Nomarski contrast.[6] In the base glass, this same technique leads to certain artifacts, e.g., premature cone crack initiation from the interface edges. Hence the two methods are complementary, and need to be examined critically in their applications to different material types.

Environmental effects in the cyclic fatigue experiments were investigated by conducting tests in "dry" nitrogen gas at relative humidity <1%, in "air" consisting of moisturized nitrogen vapor at relative humidity 50%, and in water.

Disks of diameter 35 mm and thickness 3 mm were cut and polished for biaxial flexure tests in order to measure strength degradation from the cyclic contacts. Hertzian contacts were made at the center of each polished surface for a specified number of cycles n, at a peak load P = 500 N, and frequency f = 10 Hz. Some specimens were left unindented for measurements of "laboratory" strengths. The flexure tests were conducted using a flat circular punch of diameter 6 mm on a three-ball support of diameter 22 mm. A drop of silicon oil was placed on the indentation sites prior to flexure, and the tests conducted in rapid loading (<50 ms failure time) to minimize effects of slow crack growth from environmental moisture. All broken specimens were examined to ensure that the fracture originated from the indentation sites.

III. RESULTS

A. Microscopic observations of subsurface damage

The evolution of Hertzian-induced damage with increasing number of cycles in the base glass is shown in the sequence of section views in Fig. 1, at fixed peak load P = 500 N and frequency f = 10 Hz, in air. The classical cone crack geometry[9–11] is apparent. Significant acoustic emission was heard at cone crack pop-in, enabling one to determine when (or whether) that event occurred in each test. Initiation of the cones occurred from small pre-existing surface flaws, in our

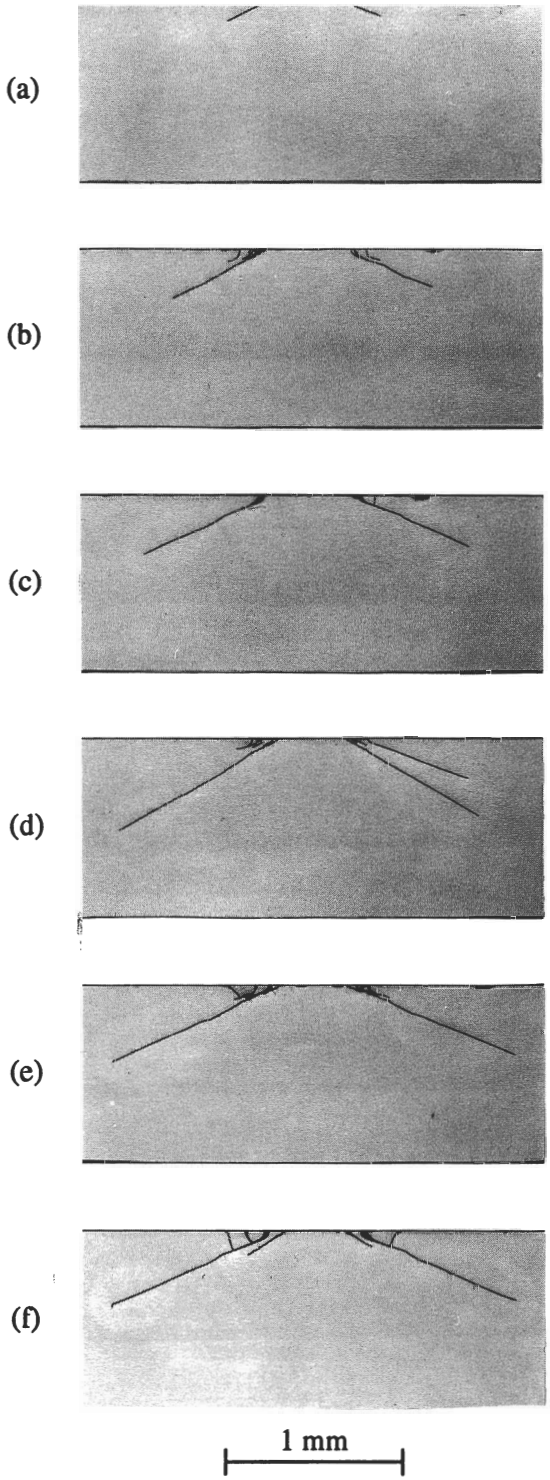

FIG. 1. Section-and-etch specimens showing growth of cone cracks with cyclic Hertzian contact in base glass, in air (relative humidity 50%). Only section views are included. Number of cycles n: (a) 10^0, (b) 10^1, (c) 10^2, (d) 10^3, (e) 10^4, and (f) 10^5. Tungsten carbide (WC) sphere radius $r = 3.18$ mm, load $P = 500$ N, and frequency $f = 10$ Hz. Optical micrographs of gold-coated sections, reflected polarized illumination.

glass presumably from polishing damage. Small polishing flaws typically have a wide distribution in size and location, leading to a strong stochastic element in the critical load for pop-in.[12] At the fixed peak load used here in our cyclic tests, the chance of pop-in was about 40% during the first 10 cycles, and about 55% during the full 10^5 cycles. Figure 1 represents an uncommon run in which all tests in the sequence produced cracks. Once pop-in did occur, the crack size was relatively reproducible. Given this, it is apparent from Fig. 1 that the cone crack does extend steadily, if slowly, with number of cycles. In this case the extension is attributable directly to slow crack growth.[13]

An analogous sequence for the crystallized glass-ceramic is shown in Fig. 2, again at fixed peak load $P = 500$ N and frequency $f = 10$ Hz, in air. Both half-surface and section views are shown in this case. The

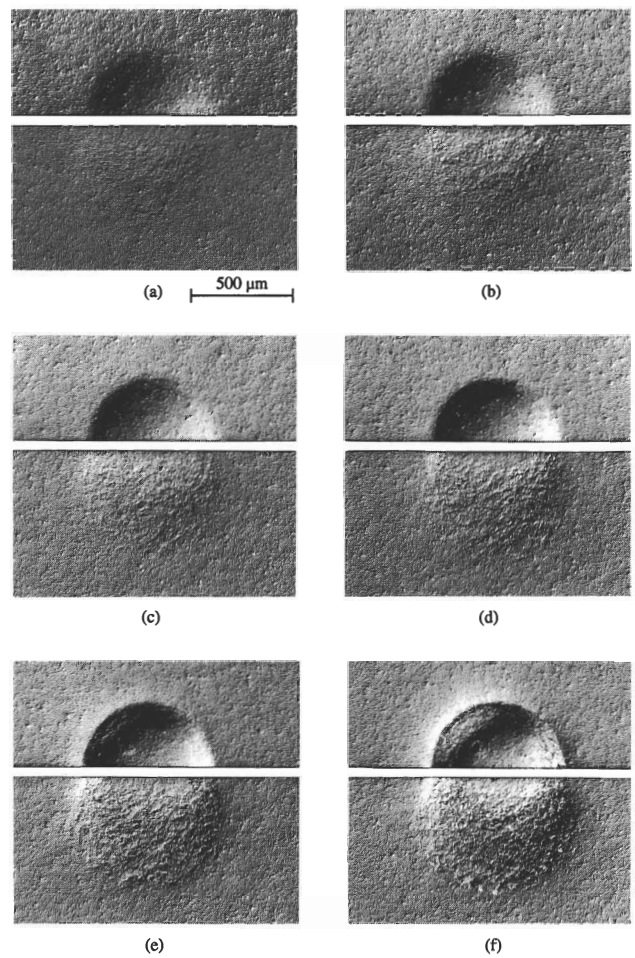

FIG. 2. Bonded-interface specimens showing subsurface damage accumulation with cyclic Hertzian contact in Macor glass-ceramic, in air. Half-surface (top) and section (bottom) views. Number of cycles n: (a) 10^0, (b) 10^1, (c) 10^2, (d) 10^3, (e) 10^4, and (f) 10^5. WC sphere radius $r = 3.18$ mm, load $P = 500$ N, and frequency $f = 10$ Hz. Optical micrographs of specimens gold-coated and viewed in Nomarski interference illumination.

damage pattern is altogether different, taking the form of a distributed damage zone immediately below the contact area.[1] In contrast to the cone cracks in the base glass, the damage patterns after a given number of cycles were highly reproducible from run to run. This reproducibility is attributable to the homogeneity of the mica second-phase microstructure, the apparent source of damage initiation. In Fig. 2, the indentation depression on the surface, and the size and intensity of the subsurface damage on the section, increase steadily with number of cycles. Relatively little acoustic emission was recorded during cycling, confirming an absence of any abrupt macroscopic fracture event in the glass-ceramic.

Figure 3 shows the results of comparative tests on the glass-ceramics run at the same peak loads and air environment as Fig. 2, but with different temporal characteristics in the cycling. In Fig. 3(a), we show the damage accumulated at static load held at peak value for a duration 1000 s. By comparison, the equivalent pattern in Fig. 3(b) obtained in cycling over $n = 1000$ cycles at frequency $f = 1$ Hz, i.e., over the same test duration, shows substantially heavier damage. This suggests a strong mechanical component in the fatigue, from some internal dissipative mechanism.[6] Figure 3(c) shows a comparable damage pattern over the same number of cycles, but now at $f = 10$ Hz, corresponding to a shortened test duration 100 s. The subsurface damage is slightly greater in Fig. 3(b) than in Fig. 3(c), suggesting a secondary chemical effect. This result implies penetration of moisture into the subsurface region, either through a continuous network of microfractures or through the adhesive at the bonded interface.

The effect of chemistry is revealed more directly by cyclic tests in different environments, Fig. 4. Tests are again run as in Fig. 2, over $n = 1000$ cycles, in (a) dry nitrogen, (b) air, and (c) water. Acceleration of damage from increasing moisture content is clearly apparent. There are signs of material detachment at the subsurface zone border in Figs. 4(b) and 4(c). The enlargement of region A in Fig. 4(b) shown in Fig. 5 confirms microfracture linkage in this region.

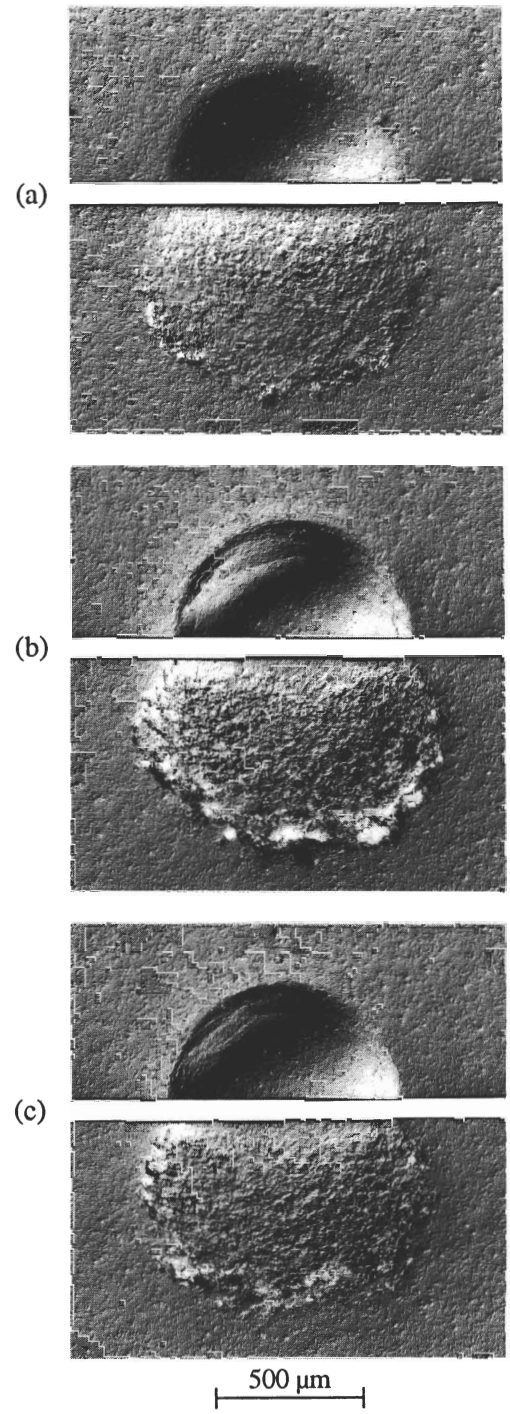

FIG. 3. Bonded-interface specimens showing change in subsurface Hertzian fatigue damage in Macor glass-ceramic with different loading time history, in air. Half-surface (top) and section (bottom) views. WC sphere radius $r = 3.18$ mm, load $P = 750$ N. (a) Held at static peak load for 1000 s; (b) cyclic loading, $n = 10^3$ at frequency $f = 1$ Hz; (c) cyclic loading, $n = 10^3$ at $f = 10$ Hz. Optical micrographs of specimens gold-coated and viewed in Nomarski interference illumination.

B. Load-displacement tests

Load-point-displacement curves over 10 cycles at peak load $P = 1000$ N and frequency $f = 1$ Hz are plotted for the base glass and glass-ceramic in Fig. 6. For an ideal Hertzian elastic contact, the following nonlinear relation between applied load P and distance of mutual approach u applies[14]:

$$u = [(4kP/3E)^2/r]^{1/3} \quad (1)$$

where E is Young's modulus (77 GPa for base glass, 63 GPa for Macor glass-ceramic) and k is an indenter/specimen elastic coefficient (for tungsten carbide indenter, 0.57 on Macor, 0.55 on base glass). Accordingly we

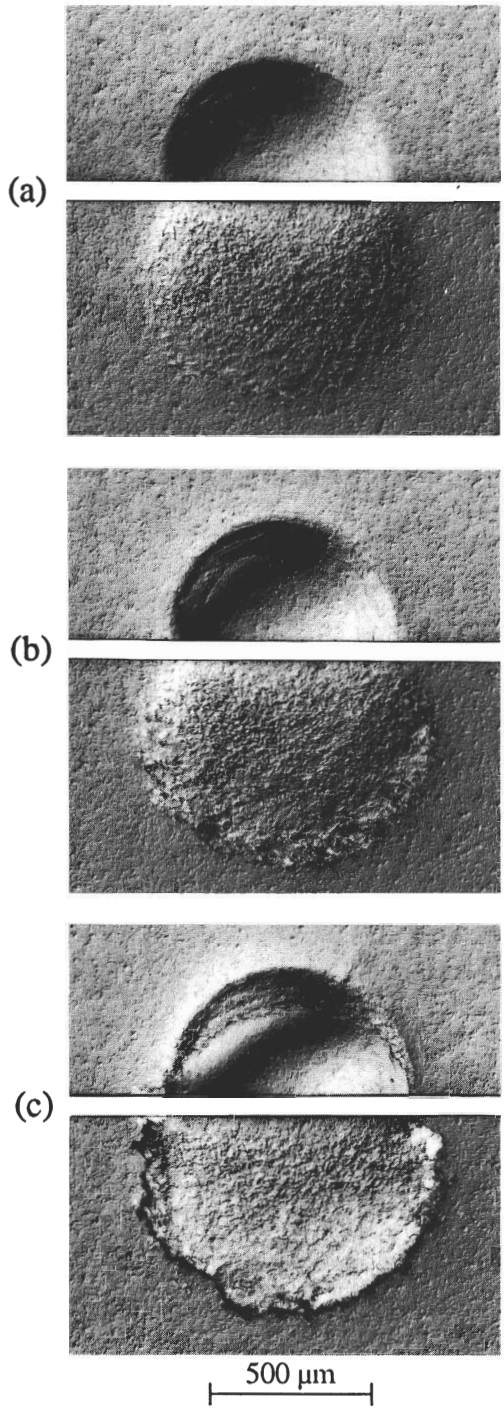

FIG. 4. Bonded-interface specimens showing change in subsurface Hertzian fatigue damage in Macor glass-ceramic with different test environment: (a) nitrogen, (b) air (relative humidity 50%), and (c) water. WC sphere radius $r = 3.18$ mm, load $P = 750$ N, number of cycles $n = 10^3$, and frequency $f = 1$ Hz. Optical micrographs of specimens gold-coated and viewed in Nomarski interference illumination.

plot the data as $P^{2/3}$ vs u, so that any departure from ideal Hertz contact may be seen as a deviation from a straight line.

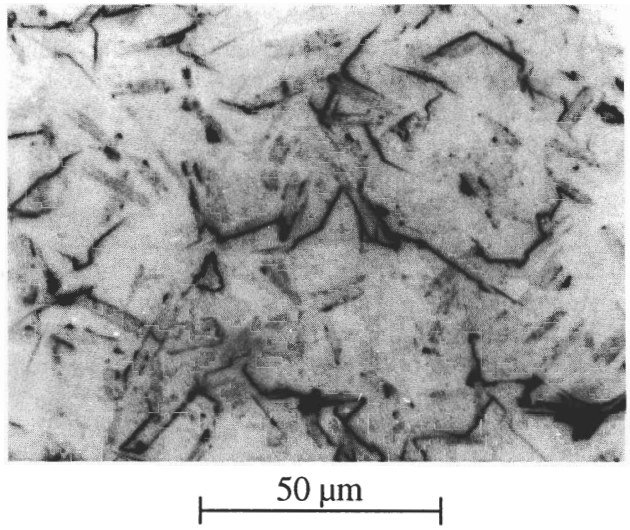

FIG. 5. Enlarged optical micrograph of region A in Fig. 4(b), showing the nature of fatigue damage in Macor glass-ceramic. Microcrack formation and coalescence are apparent at the mica flakes.

For the base glass, Fig. 6(a), the response follows the ideal straight line behavior up to $P \approx 500$ N, when the first cone crack pops in. Beyond that point the material becomes more compliant and the curve bends over. Note, however, that the hysteresis is virtually negligible over the 10 test cycles, indicating little or no energy dissipation or residual strain. Cone crack formation and closure is a relatively conservative process.[15,16]

The response for the glass-ceramic, Fig. 6(b), is quite different. Nonlinearity occurs earlier in the loading, reflecting the relative "softness" of the contact.[1] Most distinct is the pronounced hysteresis, particularly in the first cycle. This hysteresis reflects the presence of strong internal friction in the glass-ceramic microstructure, associated in our material with the mica flakes or their interfaces with the matrix. We note the presence of a substantial residual displacement, ≈ 5 μm, on completion of the first cycle, consistent with the observation of permanent contact depressions in the surface views of Fig. 2–4. This residual displacement increases with further cycling, indicating an ever-continuing micromechanical fatigue process. Whereas the existence of internal friction is incontrovertible in Fig. 6(b), we may rule out any deleterious contributions on the fatigue from heating, at least at the frequencies used in our tests, for otherwise one would expect more damage with increasing frequency; this is just opposite to what we saw in Fig. 3 (Sec. III. A).

C. Strength degradation

Figures 7(a) and 7(b) plot the results of strength degradation tests on base glass and glass-ceramic specimens subjected to cyclic Hertzian contacts at $P =$

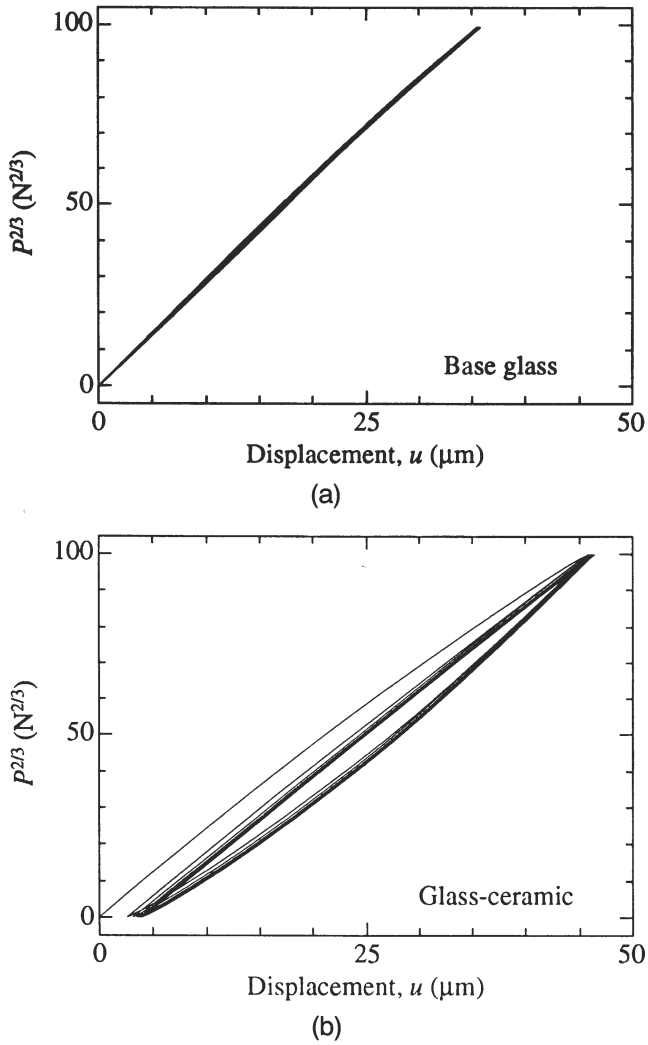

FIG. 6. Indentation load-point-displacement curves, for first 10 loading/unloading cycles: (a) base glass and (b) Macor glass-ceramic. Tests in air at load $P = 1000$ N, WC sphere radius $r = 3.18$ mm, and frequency $f = 1$ Hz. Note relatively large hysteresis in the glass-ceramic.

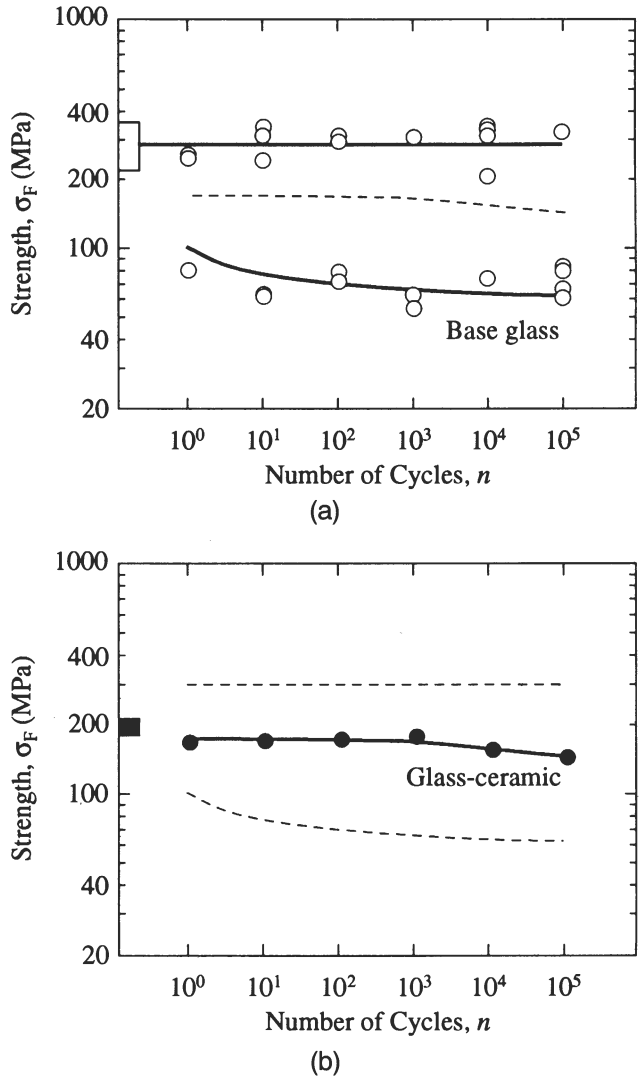

FIG. 7. Strength as a function of number of indentation fatigue cycles for (a) base glass and (b) Macor glass-ceramic. Data points for base glass are from individual breaks, for glass-ceramic means from 4 to 6 breaks (size of standard deviation error bars is smaller than symbols). Boxes at left axis represent means and standard deviations. Solid curves are data fits (see text). Dashed curves in (a) and (b) are comparison replots of solid curves from (b) and (a), respectively. Cyclic fatigue tests in air, WC sphere radius $r = 3.18$ mm, load $P = 500$ N, and frequency $f = 10$ Hz.

500 N, frequency $f = 10$ Hz, in air. Control tests on unindented specimens (box areas at left axis on the diagrams) indicate that although the glass-ceramic has a lower laboratory strength, it is also more resistant to catastrophic degradation.

In the case of the base glass, Fig. 7(a), the strength shows considerable scatter. The data divide into two bands, the upper band representing specimens *without* cone cracks, the lower band specimens *with* cone cracks (recall from Sec. III. A that the chance of cone crack pop-in through the duration of the cyclic test is just over one half). Solid curves are fits to the data. The upper curve is plotted as a horizontal line, presuming no degradation from the contacts. The lower curve is computed from a Griffith strength relation in terms of measured cone crack dimensions (e.g., from Fig. 1), normalized to a single-cycle strength $\sigma_F = 100$ MPa at $n = 1$ (Ref. 17); as indicated in Sec. III. A, this lower curve is consistent with ordinary slow crack growth in the base glass. The dashed curve from the glass-ceramic data fit in Fig. 7(b) is included for material comparison.

With the glass-ceramic, Fig. 7(b), the strength shows little sensitivity to number of cycles. The falloff is slight, but steady, consistent with the continuously progressive increase in damage observed in Fig. 2. In the absence of a comprehensive understanding of the underlying fatigue process in the glass-ceramic, the solid curve is plotted as a purely empirical fit. Again, dashed curves from

the base glass data fits in Fig. 7(a) are included for comparison purposes.

IV. DISCUSSION

We have demonstrated the existence of contact fatigue in a mica-containing glass-ceramic, Macor. It is appropriate now to compare and contrast the fatigue characteristics in the base glass and glass-ceramic states more closely, in the context of materials reliability.

In the base glass, the direct micrographic evidence in Fig. 1 suggests that the fatigue is due primarily to slow growth of cone cracks.[13] There is no evidence of significant hysteresis in the load-point-displacement curves during cycling [Fig. 6(a)], indicating the absence of major energy dissipative processes during the crack opening and closing.[18] Whereas cone fracture is unlikely to be a major contributor to surface removal (except perhaps in exceptional circumstances where extensive overlap occurs between adjacent contacts), it is [as we have seen in Fig. 7(a)] a major contributor to strength loss. If one could ensure that the contact loads in any practical application were to remain below the critical pop-in level, the mechanical properties of the base glass might be considered respectable. However, the stochastic element of cone crack initiation in the small-flaw domain, most evident as the scatter in Fig. 7(a), attests to the intrinsic unreliability of this material; a single severe surface flaw may be sufficient to cause irreparable loss of integrity in a finished component, leading to system failure.

The fatigue process in the crystallized glass-ceramic is of an altogether different kind, with a strong mechanical as well as chemical component. The mechanical component, manifest as the pronounced hysteresis in the load-point-displacement curves [Fig. 6(b)], appears to be associated with internal friction in a distributed subsurface damage zone, Fig. 2. From the standpoint of strength, the glass-ceramic is much more damage tolerant than its base glass counterpart: the cyclic degradation in Fig. 7(b) is relatively slight and, more importantly, steady, so the degradation is not catastrophic. (One might ultimately expect the glass-ceramic strength curve to drop below the lower glass curve in Fig. 7, because of eventual initiation of radial cracks at high loads.[17,19]) In addition, the presence of hysteresis in the load-point-displacement response means that the glass-ceramic has the capacity to absorb greater energy in particle impacts. On the other hand, the tendency for the Macor glass-ceramic to easy microfracture at the short-crack level foreshadows higher wear rates; in this context it is appropriate to recall that Macor is a machinable ceramic, specifically tailored to turn such apparent weakness to advantage.[2,3]

At the microscopic level, the fatigue mechanism in the glass-ceramic remains obscure. As discussed in our preceding paper on single-cycle damage in the same material,[1] the basic element of damage is some kind of shear fault at the mica-glass interface, or at an easy cleavage plane in the mica flake itself, with extensile microcracks[20,21] penetrating into the glass matrix during the contact unloading.[22] Frictional sliding at the shear-fault/microcrack interface is a critical factor in this description. Fatigue is therefore believed to arise from mechanical degradation of the frictional restraints.[23–25] These frictional elements are also subject to chemical degradation, specifically from entrant water. More work remains to be done on the elaboration of these micromechanisms.

This last point is especially relevant to the microstructural design of glass-ceramics for specific applications. What is the role of the scale and volume fraction of the mica flakes, and the mica/glass thermal-expansion and elastic mismatch, in the frictional fatigue process? Such variables certainly have a profound effect on the short- and long-crack toughness properties of general two-phase ceramics.[26,27] Again, there is scope for further work, via tailoring of microstructural characteristics by controlled heat treatments.

ACKNOWLEDGMENTS

The authors thank F. Guiberteau and N. P. Padture for fruitful discussions. Funding was provided by the United States Air Force Office of Scientific Research.

REFERENCES

1. H. Cai, M. A. Stevens Kalceff, and B. R. Lawn, J. Mater. Res. **9**, 762 (1994).
2. C. K. Chyung, G. H. Beall, and D. G. Grossman, in *Electron Microscopy and Structure of Materials,* edited by G. Thomas, R. M. Fulrath, and R. M. Fisher (University of California Press, Berkeley, CA, 1972), pp. 1167–1194.
3. K. Chyung, G. H. Beall, and D. G. Grossman, in *Proceedings of 10th International Glass Congress, No. 14,* edited by M. Kunugi, M. Tashiro, and N. Saga (The Ceramic Society of Japan, Kyoto, Tokyo, Japan, 1974), pp. 33–40.
4. C. J. Fairbanks, B. R. Lawn, R. F. Cook, and Y-W. Mai, in *Fracture Mechanics of Ceramics,* edited by R. C. Bradt, A. G. Evans, D. P. H. Hasselman, and F. F. Lange (Plenum Press, New York, 1986), Vol. 8, pp. 23–37.
5. K. Chyung, in *Fracture Mechanics of Ceramics,* edited by R. C. Bradt, D. P. H. Hasselman, and F. F. Lange (Plenum Press, New York, 1974), Vol. 2, pp. 495–508.
6. F. Guiberteau, N. P. Padture, H. Cai, and B. R. Lawn, Philos. Mag. A **68**, 1003–1016 (1993).
7. A. G. Mikosza and B. R. Lawn, J. Appl. Phys. **42**, 5540–5545 (1971).
8. F. Guiberteau, N. P. Padture, and B. R. Lawn, J. Am. Ceram. Soc. (in press).
9. F. C. Frank and B. R. Lawn, Proc. R. Soc. London **A299**, 291–306 (1967).
10. T. R. Wilshaw, J. Phys. D: Appl. Phys. **4**, 1567–1581 (1971).

11. B. R. Lawn and T. R. Wilshaw, J. Mater. Sci. **10**, 1049–1081 (1975).
12. J. D. Poloniecki and T. R. Wilshaw, Nature Phys. Sci. **229**, 226–227 (1971).
13. A. G. Evans and E. R. Fuller, Metall. Trans. **5**, 27–33 (1974).
14. K. L. Johnson, *Contact Mechanics* (Cambridge University Press, London, 1985).
15. J. S. Williams, B. R. Lawn, and M. V. Swain, Phys. Status Solidi A **2**, 7–29 (1970).
16. G. L. Cheeseman and B. R. Lawn, Phys. Status Solidi A **3**, 951–958 (1970).
17. B. R. Lawn, E. R. Fuller, and S. M. Wiederhorn, J. Am. Ceram. Soc. **59**, 193–197 (1976).
18. B. R. Lawn, *Fracture of Brittle Solids* (Cambridge University Press, Cambridge, 1993).
19. B. R. Lawn, S. M. Wiederhorn, and H. Johnson, J. Am. Ceram. Soc. **58**, 428–432 (1975).
20. H. Horii and S. Nemat-Nasser, J. Geophys. Res. **90**, 3105–3125 (1985).
21. M. F. Ashby and S. D. Hallam, Acta Metall. **34**, 497–510 (1986).
22. B. R. Lawn, N. P. Padture, F. Guiberteau, and H. Cai, Acta Metall. **42**, 1683–1693 (1994).
23. J. C. Jaeger and N. G. W. Cook, *Fundamentals of Rock Mechanics* (Chapman and Hall, London, 1971).
24. S. Suresh and J. R. Brockenbrough, Acta Metall. **36**, 1455–1470 (1988).
25. S. Suresh, *Fatigue of Materials* (Cambridge University Press, Cambridge, 1991).
26. B. R. Lawn, N. P. Padture, L. M. Braun, and S. J. Bennison, J. Am. Ceram. Soc. **76**, 2235–2240 (1993).
27. N. P. Padture, J. L. Runyan, S. J. Bennison, L. M. Braun, and B. R. Lawn, J. Am. Ceram. Soc. **76**, 2241–2247 (1993).